

# Transparent Barrier Coatings Update: Flexible Substrates

J.T. Felts, Airco Coating Technology, Concord, CA

---

**Keywords:** Permeation barrier coatings; SiO<sub>x</sub>; Polymer substrates

---

## ABSTRACT

SiO<sub>x</sub> thin films continue to be developed for polymeric flexible substrates. During the past year significant progress has been made on plasma deposition onto PET, LDPE, BOPP and BON polymer films. In addition, the first two 1.5 meter wide plasma roll coaters were completed and installed. The current state of the roll-to-roll coating developments on BOPP, LDPE, PET and BON will be reported for the 0.3 meter wide roll coater, R9, the 0.66 meter wide roll coater, Flex-1, along with data from the 1.5 meter wide coater, Flex-3, operations. The paper will then focus on a new stretch tester that measures oxygen transmission of stretched SiO<sub>x</sub> coated polymers. Data from the plasma coatings along with comparative measurements made on commercially available evaporated products clearly shows a strong inverse relationship between the SiO<sub>x</sub> coating thickness and the onset of failure (strain) S<sub>f</sub>. Plasma coatings were stretched to 11.9% before failure occurred while the evaporated materials degraded at S<sub>f</sub>=2-3%. The stretch tester is a repeatable technique to assess the convertibility of the SiO<sub>x</sub> coated polymers and to make quantitative assessments between competitive materials. A model is also presented outlining the key parameters in achieving gas barrier properties with thin SiO<sub>x</sub> and AlO<sub>x</sub> coatings.

## INTRODUCTION

Thin film gas diffusion barriers were introduced to the packaging industry through aluminum metallization of thin polymeric webs as early as 1959. Aluminized gas diffusion barriers have proven useful and their acceptance has grown steadily over the years. Recent trends, however, have focused on transparent thin film barrier materials that will give the barrier performance of aluminized polymers without the opaque nature of a metal. Furthermore, the transparent webs would be microwaveable and would allow direct measurement with metal detectors on fabricated packages. Several approaches for depositing transparent coatings on polymers are currently being commercialized including the evaporation of silicon monoxide, aluminum and magnesium in oxidizing atmospheres as well as the plasma deposition of silicon oxides and nitrides.

The commercialization of transparent gas diffusion barrier coatings is not a simple matter of depositing the barrier coating, but instead involves the complex interaction between the

thin coating, the base polymer film and the many possible routes of conversion into the final package. The conversion process offers many obstacles to the successful commercialization of transparent barrier coating and will determine the market acceptance of these coatings. This paper focuses on the mechanisms that limit the fundamental gas diffusion barrier properties of the coating material and focuses on a stretch test method that directly measures the durability of the coating/polymer structure. The stretching system was developed at Airco Coating Technology utilizing a Modern Controls single station oxygen transmission measurement instrument. The film was clamped to a fixture on a moving stage and also to a fixture permanently attached to the Mocon instrument top plate. Before the film was stretched, the oxygen cell was opened, the film was then stretched and the oxygen cell closed. The new test method is presented as an improved method of quantifying the convertibility of all barrier coating/polymer products.

This paper is an extension of a previously published paper on thickness effects on thin barrier coating materials.<sup>1</sup>

## Experimental Set-up

Transparent SiO<sub>x</sub> barrier coatings were deposited onto polymeric webs by plasma decomposition of 1,1,3,3-tetramethyldisiloxane [TMDSO], oxygen and helium in a 40 kHz magnetically enhanced plasma discharge. The coatings were deposited at 50 mTorr total process pressure. Polymer substrates coated to date include poly (ethylene terephthalate) [PET], biaxially oriented polypropylene [BOPP], biaxially oriented nylon [BON] and low density polyethylene [LDPE] (**Table 1**). PET will be the focus of this paper. Three different batch roll-to-roll plasma systems were used to deposit the films; a 0.3 meter wide free-spanned roll-to-roll coater [R9], a 0.66 meter wide pilot production machine [Flex1], and a 1.5 meter wide production scale coater [Flex3] (**Figure 1**). Statistically designed experiments (SDE) were used to optimize the plasma coating process for minimum oxygen and water vapor transmission rates on each substrate material. Over the many experiments completed in all three plasma roll-to-roll systems, the significant process variables consistently included TMDSO and oxygen flows, linespeed, and power. The gas diffusion barrier plasma process was optimized for minimum transmission rates separately for each polymer substrate; the conditions that produced the best barrier were different for each substrate (**Table 1**).

**Table 1 - Oxygen and Water Vapor Transmission Rates of Plasma Coated Polymeric Substrates**

Substrate	Thickness (microns)	Oxygen Transmission (cc/m <sup>2</sup> /day)	Water Vapor Transmission (g/m <sup>2</sup> /day)
PET	12	1	1
BOPP	25	<10	2
LDPE	25	10	-
BON	12	0.6	-

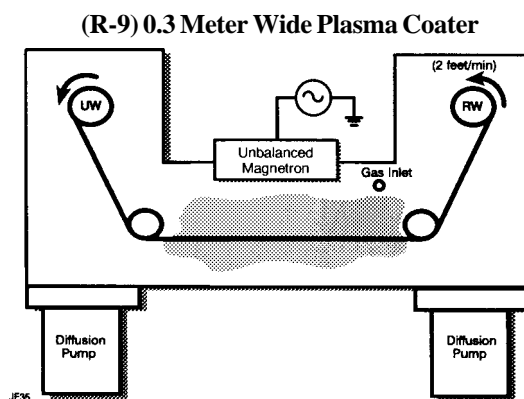
Evaporated coatings were obtained from various manufacturers and were deposited from either evaporation of SiO or Aluminum in an oxygen atmosphere. All of the evaporated coatings were deposited onto 0.5 mil thick PET. The thickness of SiO<sub>x</sub>#2 was reported to be 1600 Å, while SiO<sub>x</sub>#1 and AlO<sub>x</sub> were reported to be 600 Å.

All oxygen transmission rates were measured on Modern Controls instrumentation at ambient temperature (approximately 24° centigrade) and at 50% relative humidity. Coating thicknesses were determined from x-ray fluorescence (XRF) measurements with an ASOMA Model 200/400 benchtop unit. Both the Mocon and ASOMA instruments were calibrated on a weekly basis to insure repeatable measurements.

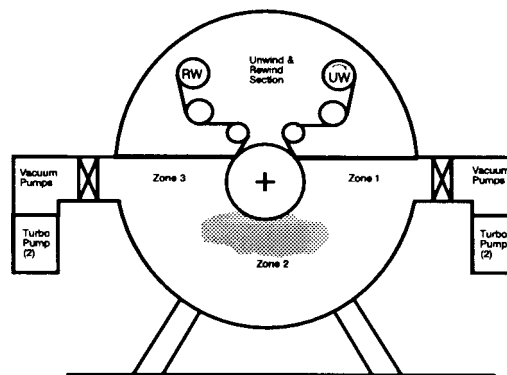
The durability of the as-deposited polymer-thin film structure was evaluated using a new system which controllably stretched the structure and measured oxygen transmission rate as a function of the percent stretch. The stretching system (Figure 2) was developed at Airco Coating Technology utilizing a Modern Controls single station oxygen transmission measurement instrument. A Newport optical stage with a micrometer was used to stretch the coated polymer film. The film was clamped to a fixture on the moving stage and also to a fixture permanently attached to the Mocon instrument top plate. The oxygen cell area was 50 cm<sup>2</sup> and was centered in the middle of the 5" wide web strip. Additionally, the cell height was carefully matched to the web position to minimize additional stretching from the clamping action of the cell. In all cases, the films were mounted so that the unstretched dimension was 17.46 cm and were stretched in 0.127 cm increments between oxygen transmission rate measurements. Before the film was stretched, the oxygen cell was opened, the film was then stretched and the oxygen cell closed. The vacuum grease used in the seal between the film and the cell was pulled into the measurement area when the films were stretched beyond 4%. A minimum of 3 separate samples were stretched in each case (except where noted) and the average oxygen transmission rate taken for the three measurements at each stretch condition.

**Experimental Results**

To date, evaporation of SiO<sub>x</sub> coatings has been mainly onto PET substrates. The plasma work reported herein, however, has begun to shift focus from PET to non-PET materials, spe-



**(FLEX-1) 0.66 Meter Wide Prototype Web Coater**



**(FLEX-3) 1.5 Meter Wide Production Scale Plasma Coater**

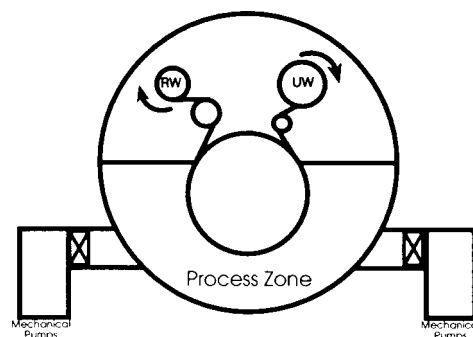


**Figure 1 - Plasma Roll Coaters**

## Developed New Testing Apparatus

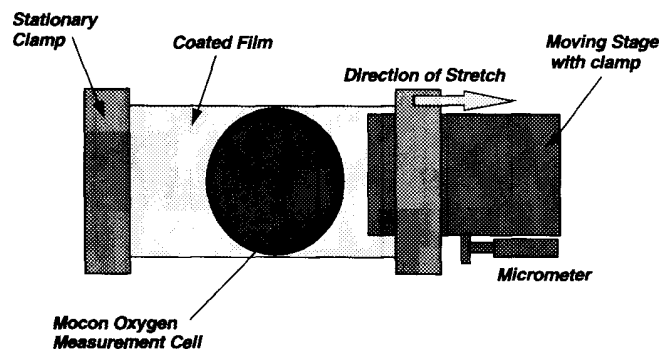


Figure 2 - Oxygen Transmission/Stretching Apparatus

cifically BOPP, LDPE and BON. Since the bulk of the work has been on PET, the lowest transmission rates have been achieved on PET. The fact that oxygen transmissions of 10 cc/m<sup>2</sup>/day or less were achieved on all of these substrates was surprising, since a wider range of oxygen transmission results is reported for metallized polyester and polyolefin materials using aluminum.<sup>2</sup> The gas diffusion barrier properties achieved with SiO<sub>x</sub> (and other thin coatings on polymers like aluminum) have varied with the deposition method used as shown in **Table 2**. Additionally there were no significant differences between the minimum transmission rates that were achieved on PET in each of the 3 plasma deposition systems used in this study.

In this study, we stretched coated PET polymers produced at Airco Coating Technology and three commercially available evaporated materials. The oxygen transmission rate results as a function of the strain are presented in **Table 3** and **Figure 3**.

### Discussion

The durability of the SiO<sub>x</sub> barrier coating materials has been difficult at best to quantify. Typical testing entails mounting a polymer/SiO<sub>x</sub> structure onto a conventional Gelbo flex tester and then cycling the material through multiple wrinkling steps. Unfortunately, this test will produce pin-holes in uncoated PET films after 100 cycles and is, therefore, a very destructive test method. The principal objective of the Gelbo film

test is to determine the ability of polymeric structures to withstand subsequent processing in the converting line, and the ability of the coating/polymer structure to survive in the final laminated form. The second objective is readily achievable once the coating/polymer structure is laminated and the SiO<sub>x</sub> layer protected. In the first case, however, the Gelbo test produces highly variable results. To circumvent the problems associated with testing unlaminated material, we have developed a stretch test apparatus as described above. In this study, we stretched coated polymers produced at Airco Coating Technology and three commercially available evaporated materials. The results are presented in **Table 3** and **Figure 3**. There was a clear trend for all of the coated films: the oxygen transmission rate of each coating remained constant with increasing strain at first, then quickly degraded to >10 cc/m<sup>2</sup>/day when the coating failed. The point at which failure occurs (the failure onset strain, S<sub>f</sub>) was obtained by linear extrapolation of the curve after failure to the x-axis. Surprisingly, the plasma produced coating from the 1.5 meter wide coater had exceptional elongation properties and were stretched over 4x more than evaporated coatings before a rise in oxygen transmission rate was observed. Additionally, the plasma coating (R9930112-2) from the 0.3 meter wide research roll-to-roll coater (R9) was not as stretchable as the Flex-1 (F1930121-1) material. The R9 material was thicker (583 Å as determined by XRF measurement) compared to the Flex-1 coating (304 Å also measured by XRF measurement). To test the effect of coating thickness, a coating was made in the R9 roll-to-roll coater at 0.61 meters/minute (R9930210-4) (2x the speed from R9930112-2). The coating thickness was approximately one-half (200 Å) that of R9930112-2 and gave a much higher oxygen transmission rate prior to stretching. The material did degrade much slower than the thicker R9 coating, but degraded faster (S<sub>f</sub> = 5.9%) than the similar thickness sample from Flex-1 (S<sub>f</sub> = 8%) (**Table 3**). The difference in oxygen transmission between the two plasma samples shows that absolute oxygen transmission will effect the stretchability of the SiO<sub>x</sub> coating. The effect of thickness shown in the R9 samples was shown further in the plasma produced Flex-3 sample (F3930323) which was 130 Å thick (as measured by XRF). The failure onset strain, S<sub>f</sub> of the Flex-3 sample was 11.9% (**Figure 4**). The thickness of all of the samples were plotted versus the stretching failure point of each mate-

Table 2 - Oxygen Transmission Rates of Evaporated and Plasma Deposited SiO<sub>x</sub> Coatings

Process	Material	Thickness (Å)	O <sub>2</sub> Rate (cc/m <sup>2</sup> /day)	H <sub>2</sub> O Rate (g/m <sup>2</sup> /day)
Resistance Evaporation	SiO	600	2.2	2.5
E-Beam Evaporation	SiO	600	3.0	2.0
Plasma (Airco)	SiO <sub>2</sub>	200	1.0	1.0

NOTE: Plasma samples were all measured at Airco Coating Technology. Competitive evaporation data was taken from each competitor's publications and product brochures.

**Table 3. Table with Stretch Data - QLF® Mocon Stretching Experiment**

Sample	rometer	Tur*	Stretched	% Stretch	OXTRAN (cc/m <sup>2</sup> /day)	OXTRAN (cc/m <sup>2</sup> /day)	OXTRAN (cc/m <sup>2</sup> /day)	Average OXTR	Stdev	Stretch Failure Point (S <sub>f</sub> ) (% Stretch)
R-9 QLF/PET R9930112-2 583 Å	0		6.875	0.0000	1.337	1.479	1.446	1.421	0.07	4.50%
	1		6.925	0.0073	1.341	1.518	1.435	1.431	0.09	
	2		6.975	0.0145	1.366	1.587	1.562	1.505	0.12	
	3		7.025	0.0218	1.397	2.722	1.557	1.555	0.16	
	4		7.075	0.0291	1.517	2.703	1.64	1.620	0.09	
	5		7.125	0.0364	1.64	1.828	1.73	1.733	0.09	
	6		7.175	0.0436	1.6	2.151	1.87	1.874	0.28	
	7		7.225	0.0509	1.789	11.83	2.13	5.250	5.70	
	8		7.275	0.0582	8.02	73.4	28.99	36.803	33.38	
9		7.325	0.0655	89.2		41.2	55.200	19.80		
Flex-1 QLF/PET F1930121-1 304 Å	0		6.875	0.0000	1.92	2.01	2.03	1.987	0.06	8%
	1		6.925	0.0073	2.11	1.97	2.02	2.033	0.07	
	2		6.975	0.0145	1.88	2.01	1.91	1.933	0.07	
	3		7.025	0.0218	1.99	2.096	2.03	2.039	0.05	
	4		7.075	0.0291	2.19	2.262	2.16	2.204	0.05	
	5		7.125	0.0364	2.36	2.459	2.35	2.390	0.06	
	6		7.175	0.0436	2.57	2.325	2.61	2.502	0.15	
	7		7.225	0.0509	2.72	2.485	2.82	2.675	0.17	
	8		7.275	0.0582	2.2	2.639	3.09	2.643	0.45	
	9		7.325	0.0655	3.34	2.815	3.37	3.175	0.31	
	10		7.375	0.0727	5.91	2.037	3.25	3.732	1.98	
	11		7.425	0.0800	5.62	3.637	3.71	4.322	1.12	
	12		7.475	0.0873	6.87	12.38	10.97	10.073	2.86	
	13		7.525	0.0945	6.41	70.8	60.8	48.003	34.65	
	14		7.575	0.1018	10.45	107.2		58.825	68.41	
	15		7.625	0.1091	23.91					
16		7.675	0.1164	55.7						
SiOx #1 1600 Å	0		6.875	0.0000	1.72			1.720		2.95%
	1		6.925	0.0073	1.71			1.710		
	2		6.975	0.0145	1.82			1.820		
	3		7.025	0.0218	2.03			2.030		
	4		7.075	0.0291	2.4			2.400		
5		7.125	0.0364	24.9			24.900			
6		7.175	0.0436	74			74.000			
AlOx 600 Å	0		6.875	0.0000	3.59	3.86	2.88	3.44	0.51	2.19%
	1		6.925	0.0073	3.66	3.90	3.51	3.69	0.2	
	2		6.975	0.0145	5.14	4.10	3.4	4.21	0.88	
	3		7.025	0.0218	5.40	4.40	3.73	4.52	0.86	
	4		7.075	0.0291	6.03	5.20	5.04	5.42	0.53	
	5		7.125	0.0364	6.79	9.5	6.9	7.73	1.53	
	6		7.175	0.0436	20.63	41.6	38.8	33.67	11.39	
7		7.225	0.0509	98.7	116.7	123.8	113.07	12.94		
SiOx #2 600 Å	0		6.875	0.0000	2.6	4.09		3.345	1.05	2.00%
	1		6.925	0.0073	2.662	4.5		3.581	1.30	
	2		6.975	0.0145	2.68	6.8		4.740	2.91	
	3		7.025	0.0218	2.936	11.77		7.353	6.25	
	4		7.075	0.0291	3.4	35.78		19.590	22.90	
	5		7.125	0.0364	11.67	62.4		37.035	35.87	
6		7.175	0.0436	62			62.00			
R-9 QLF/PET R9930210-4 200 Å	0		6.875	0.0000	8.9	9.91	7.9	8.903	1.01	5.9%
	1		6.925	0.0073	10.7	10.16	8.8	9.887	0.98	
	2		6.975	0.0145	11.9	11.77	9.6	11.090	1.29	
	3		7.025	0.0218	13.3	12.97	10.5	12.257	1.53	
	4		7.075	0.0291	13.3	14.11	10.7	12.703	1.78	
	5		7.125	0.0364	14.6	16.54	11.9	14.347	2.33	
	6		7.175	0.0436	16.8	18.25	13.6	16.217	2.38	
	7		7.225	0.0509	19.1	21.05	14.5	18.217	3.36	
	8		7.275	0.0582	22.98	23.2	17.2	21.127	3.40	
	9		7.325	0.0655	23.8	24.0	19.2	22.333	2.72	
	10		7.375	0.0727	27.1	21.9	21.5	23.500	3.12	
	11		7.425	0.0800	32.6	25.4	26.9	28.300	3.80	
	12		7.475	0.0873	59.6	31.4	46.1	45.700	14.10	
13		7.525	0.0945		48					
Flex-3 QLF F3930323 130 Å	0		6.875	0.0000	2.12	2.039		2.080	0.06	11.90%
	1		6.925	0.0073	1.99	1.878		1.934	0.08	
	2		6.975	0.0145	2.15	2.03		2.090	0.08	
	3		7.025	0.0218	2.33	2.14		2.235	0.13	
	4		7.075	0.0291	2.48	2.33		2.405	0.11	
	5		7.125	0.0364	2.79	2.52		2.655	0.19	
	6		7.175	0.0436	2.54	2.73		2.635	0.13	
	7		7.225	0.0509	2.79	3.2		2.995	0.29	
	8		7.275	0.0582	3.01	3.23		3.120	0.16	
	9		7.325	0.0655	3.31	3.6		3.450	0.20	
	10		7.375	0.0727	3.59	3.94		3.765	0.25	
	11		7.425	0.0800	4.04	4.43		4.235	0.28	
	12		7.475	0.0873	4.48	5.19		4.835	0.50	
	13		7.525	0.0945	4.99	5.87		5.430	0.62	
	14		7.575	0.1018	5.53	7.92		6.725	1.69	
	15		7.625	0.1091	6.4	11.3		8.850	3.46	
	16		7.675	0.1164	10.3	12.4		11.350	1.48	
	17		7.725	0.1236	22.3	14		18.150	5.87	
	18		7.775	0.1309	45.4	19.8		32.600	18.10	
	19		7.825	0.1382		43.5		43.600		
20		7.875	0.1455		84.6		84.600			

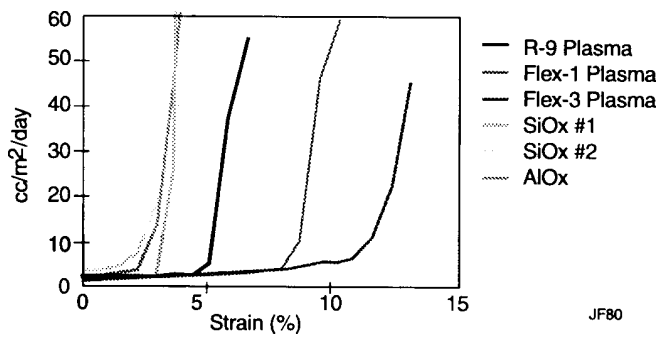


Figure 3 - Stretch Results of Evaporated and Plasma Coatings

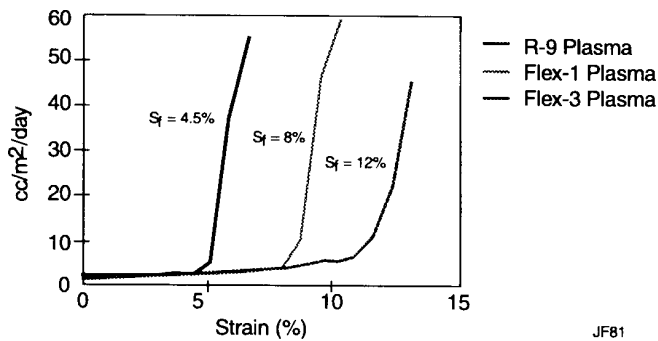


Figure 4 - Plasma Coater Comparison

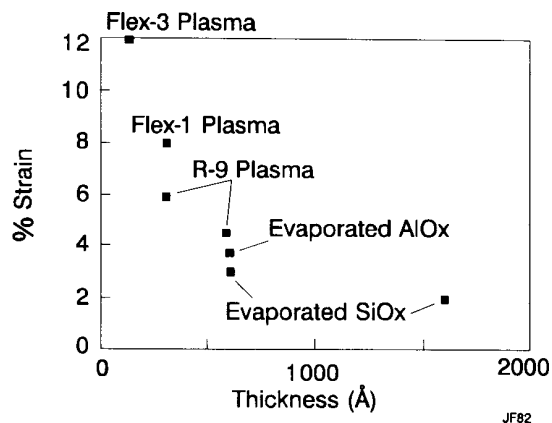


Figure 5 - Thickness vs. Strain

rial (Figure 5).<sup>4</sup> Three samples examined in this study had the same thickness (600 Å): plasma produced SiO<sub>x</sub>, evaporated SiO<sub>x</sub> and evaporated AlO<sub>x</sub>. The early onset of barrier failure for stretched evaporated materials ( $S_f = 2 - 3\%$ ) is consistent with market reports that the evaporated materials perform poorly in the conversion processes and are very susceptible to damage. The plasma produced coatings, however, survived significant strain ( $S_f = 4.5\%$ ), with the amount of elongation increasing with decreasing thickness. The strong inverse relationship between the thickness of thin coatings and their failure point ( $S_f$ ) on extensible substrates was shown previously by Hosaka

who studied evaporated gold coatings (600-3200 Å).<sup>3</sup> Increasing the stretch point requires reducing the coating thickness, hence there is a trade-off between optimum gas barrier properties and the optimum extensibility of the coating. The differences between evaporation and plasma processes in obtaining barrier for a given thickness indicates that the performance of each coating is limited by the deposition method (evaporation or plasma) (Figure 5).

The “knee” in the stretch/oxygen transmission rate curve for the stretched coating/substrate structure is assumed to be the point at which the coating begins to crack (cohesive failure), since the increase in oxygen transmission rate is due to the creation of defects (in this case cracks induced in the coating due to the large difference in elongation properties of the substrate and the thin coating) in the thin coating. The rate at which the transmission rate of the coating degrades after the onset of cracking indicates the relative adhesion between the coating and the base film.<sup>4</sup> Table 4 lists the slopes of lines fit to each data set. Two lines were fit to each stretch set, the first to the region where the coating maintained gas barrier properties, the second to the region where the thin coating failed. The slope of the line after  $S_f$  is reached is indicative of the rate of failure, and therefore the degree of cracking (defects). Once failure was reached in the coatings, there were no significant differences between the plasma produced coatings and the SiO<sub>x</sub>#2 samples except in the case of the thin R9 sample. The degradation of SiO<sub>x</sub>#1 and AlO<sub>x</sub>, however, was significantly worse. Based on the coarse relationship between adhesion and the indirect measurement of cracking in the stretch test, we can only conclude that the SiO<sub>x</sub>#1 and AlO<sub>x</sub> samples had significantly worse adhesion. Thus it is not clear what is different between these coatings. What is clear is that some other material properties are different between the coatings, and the differences influence both the oxygen transmission rate and  $S_f$ . The extreme difference between the AlO<sub>x</sub> sample and the rest of the data is in-line with market reports that the AlO<sub>x</sub> coatings are difficult to convert into flexible packages. If we consider both the degree to which the coatings were strained before failure and the rate of failure, a more representative estimate can be made relative to the adhesion of each sample. In this case, it is easy to see that the plasma coatings had significant adhesion to the PET substrate, while the evaporated coatings all had much poorer adhesion.

To quantify the differences in adhesion between each coating, the cracking pattern of each material at failure must be determined. The films were stretched to failure and the cracking patterns were photographed with a scanning electron microscope (SEM). In each case the samples were sputter coated with a thin gold coating to assure that the sample surface would not charge during the analysis. The cracking patterns were not significantly different within each deposition method; that is, the evaporated coatings all gave similar results. The plasma coatings gave similar results as well, although different than the evaporated samples. Representative photos are shown

in **Figure 6**. The cracking pattern for the plasma coatings exhibited a regular fine structure of parallel cracks indicating good adhesion,<sup>4</sup> while the evaporated coatings exhibited a coarse nonparallel structure which indicates poor adhesion.<sup>4</sup> Furthermore, upon examination of the SEM photos, the evaporated coating seems to be delaminating from the base PET film in the areas where it had cracked and in some cases, the coating had “flaked” off of the base film.

The flaking of the evaporated coating from the polymer suggest that the evaporated coatings formed a simple mechanical bond to the base film (this was clearly shown when the coating flaked off of the PET base film). Given the greater stretchability of the plasma coating and the cracking pattern at failure, the plasma coating appears to be forming a chemical bond to the PET, perhaps by nucleating at oxygen sites of the PET backbone. The chemical bond is of particular importance when considering the extreme environment of conversion processes, namely lamination (both adhesive and extrusion). Additionally, as the SiO<sub>x</sub> coating thickness was reduced (that is the deposited thickness of the gas barrier material), the elongation point was also extended. Therefore, to increase the elongation of the SiO<sub>x</sub> coating, either increases in the coating/substrate adhesion or decreases in the coating thickness are required. Since the stretching is related to the processability of the coating/substrate structure in converting operations (laminating, printing etc.), the adhesion and thickness must be included when optimizing the total coating properties, not simply optimizing the coating stoichiometry<sup>5</sup> or deposition method. A more complete model of thin transparent gas barrier materials can now be described.

Previously we have reported on the effect of thickness of thin film coatings on the oxygen transmission rate on polymeric webs.<sup>1</sup> There were 3 distinctive oxygen transmission regions observed: the nucleation region, the so-called classical region

and the damage region (**Figure 7**). The model, however, did not address why the minima in the transmission rate/thickness curve was not zero (a perfect barrier) and what additional coating parameters affect the gas transmission rate. From the current understanding of the gas barrier properties of these coatings and our work on coating substrates other than PET, we expect that the offset is due to coating defects (pinholes) resulting either from debris present on the substrate prior to coating or created during the deposition process. Previous work on palladium coatings evaporated onto polyethylene clearly showed the effects of such defects on the gas transmission properties.<sup>6</sup> Additionally, the importance of defects in chemical vapor deposited SiO<sub>2</sub> coatings on the oxygen transmission rate was shown clearly by Ing et al.<sup>7</sup> The effect of defects on the gas transmission properties become significant after the optimal coating chemistry is achieved. The coating chemistry determines the bulk gas diffusion rate in the thin coating and should (if there are no defects) determine the ultimate gas barrier properties of a coated polymer. In this paper we have shown that the coating/substrate degree of stretchability to failure is inversely related to the thickness of the deposited coating (**Figure 5**). The point of failure in our stretch test indicates the durability of the coating/substrate structure which is indicative of the convertibility of the completed structure. Additionally we have shown that adhesion significantly impacts the durability of the coating/substrate structure. Based on our previous work and these new findings, the key variables in forming a transparent gas barrier coating are:

- Deposition Method (plasma or evaporation)
- Coating chemistry
- Thickness
- Adhesion
- Defects (pinholes)

**Table 4 - Failure region of the stretched samples.**

Coating ID	Process Type	Slope of Line fit to Failure region	Degree of Fit of Line (Perfect fit = 1.0)
R-9 QLF (1/2 thickness)	Plasma	15.6	0.95
R-9 QLF	Plasma	26.2	0.96
Flex-1 QLF	Plasma	27.5	0.96
Flex-3 QLF	Plasma	29.0	0.96
SiO <sub>x</sub> #2	Evaporation	29.2	0.99
SiO <sub>x</sub> #1	Evaporation	49.3	0.98
AlO <sub>x</sub>	Evaporation	72.1	0.96

Note that the deposition method and the coating chemistry are highly interdependent and difficult to separate. A conceptual model that includes these key variables and their relationship to oxygen transmission rate is shown in **Figure 8**. The model shows that each gas barrier materials properties are determined first by selecting (optimizing) for the optimal chemistry. In the case of plasma produced coatings, this depends on the input gas type and ratio as well as the equipment configuration and power levels selected. For the optimal chemistry, there is a strong dependence between the thickness of the coating and the gas barrier properties. For very thin coatings, the substrate

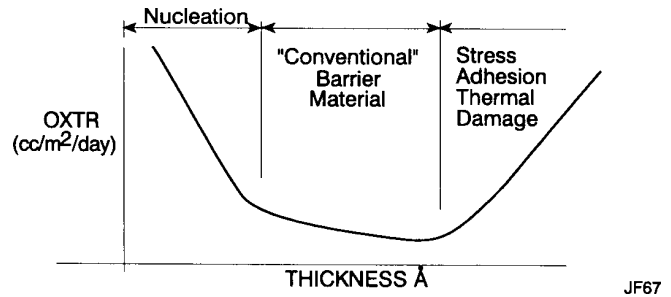
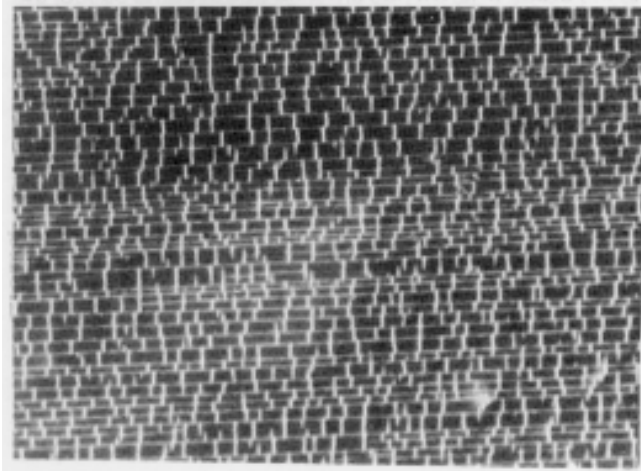


**Figure 7 - Thickness/Oxygen Transmission Rate Model**



**Plasma Coating @ 15% stretch (R-9)**

20 µm



**Evaporated Coating @ 15% stretch (SiOx #1)**

**Figure 6 - SEM micrographs of stretched plasma and evaporated coatings**

is not completely covered with the coating and hence the coating has poor barrier properties. As the coating thickness is increased, the conformal coverage is increased and the gas barrier properties improve up to a critical thickness where the thermal load of the process, internal stresses of the coating and poor adhesion begin to affect the gas transmission properties eventually leading to a failure of the coating/substrate structure.<sup>1</sup> The ultimate gas barrier performance is dependent on the number and type of defects present on the substrate and generated within the coating process. For example, coating build-up on shields within the evaporation process will eventually crack and “flake-off” of the shielding in the form of particles and flakes. If this debris contacts the substrate prior to coating, a defect (pinhole) will result causing a high transmission path for the diffusing gas. For a given chemistry, adhesion and count, the durability of the deposited coating is inversely dependent on the coating thickness as shown above.

Based on the conceptual model, the optimal chemistry must be determined (In most cases the chemistry will directly influence the adhesion) and then the minimum coating thickness determined. In all cases, the defects on the web and from the process must be minimized. In the case of plasma processing, all of the key variables (except for debris present on the web before processing and debris generated by the coater) are controllable from the process inputs of gas type and composition, power, and linespeed. Unfortunately, evaporation can only influence some of the variables through process inputs given the limitations of the evaporation process, mainly the input power and linespeed since the coating material is fixed in each case. An additional degree of freedom can be added to evaporation by adding a process gas such as oxygen to influence the chemistry of the growing coating. If one adds a process plasma in addition to the process gas for evaporation, there is a possibility of controlling all of the input parameters that will influence the key coating variables. In all cases, the web surface that is presented to the deposition zone must be as clean as possible and, the debris generated within the coater from moving parts and coating build-up must be minimized.

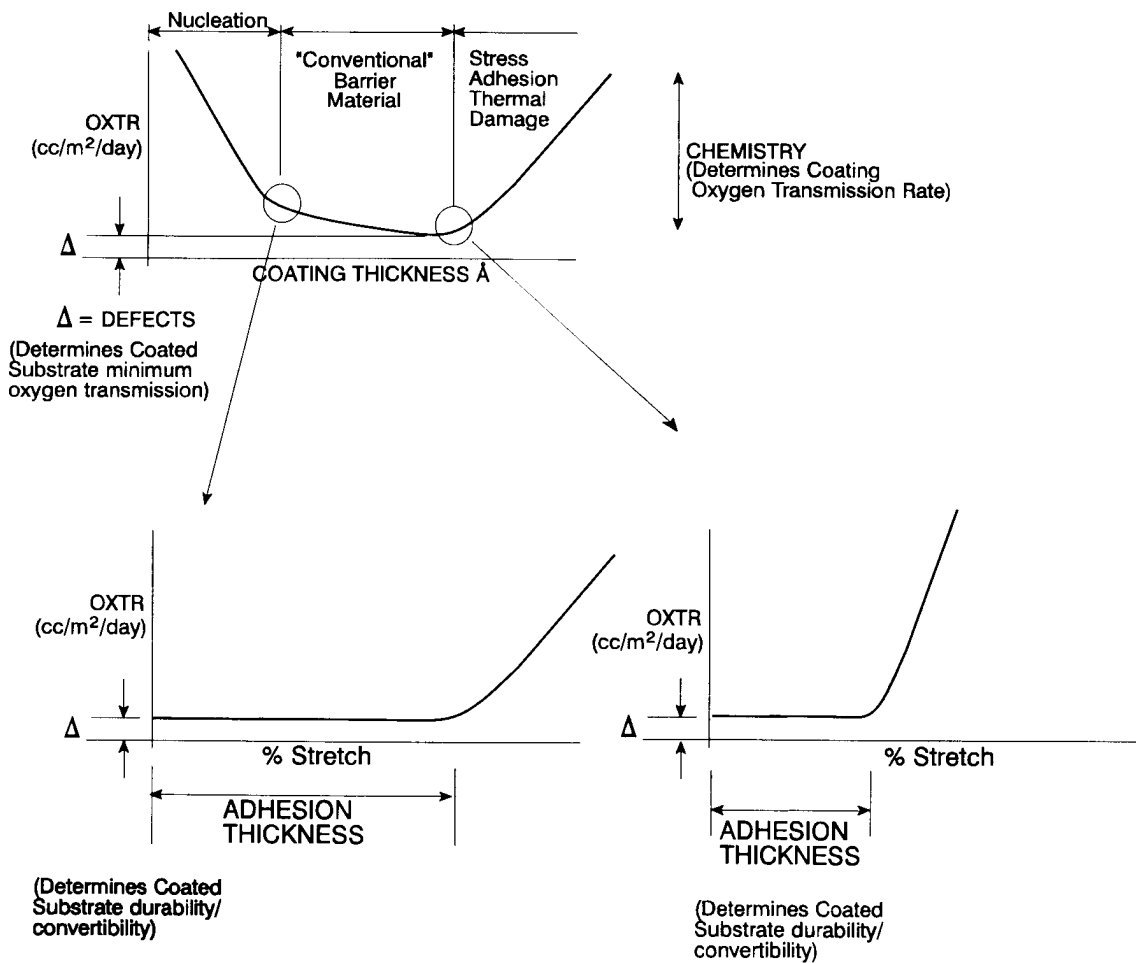
### CONCLUSIONS

Data was presented that showed oxygen transmission rates below 10 cc/m<sup>2</sup>/day can be achieved independent of the substrate material. The lack of substrate dependence on the oxy-

gen transmission rate indicates that the coated substrates' ultimate barrier is not limited by the substrate, but is limited by coating chemistry, deposition method, coating thickness and defects. The importance of adhesion was shown when polymer/thin film structures were stretched. Good adhesion must be achieved in order to improve the durability of the coating/substrate structure and aid in successful conversion to final package applications. The plasma deposited coatings demonstrated superior stretch performance relative to the evaporated coatings. Furthermore, decreasing coating thickness was shown to increase the extent that the coating can be stretched before losing oxygen barrier properties. It must be noted that the very high values of  $S_f$  for the plasma coatings seems very unusual and suggests some unique material properties. The stretch tester presented is a good indicator of the durability of thin coating/polymer structures and can be used to quantitatively differentiate between coating types and thicknesses.

## REFERENCES

1. J. Felts, *Society of Vacuum Coaters 34th Annual Technical Conference Proceedings*, March 16-23, 1991.
2. R. Kelly, *Barrier Pack 1990 Conference Proceedings*, London, England, The Packaging Group Inc. New Jersey, USA.
3. T. Hosaka, *J. Vac. Soc. Jpn.* 31, 687 (1988).
4. P. Wajciechowski and M. Mendolia, *Physics of Thin Films*, Edited by M. Francombe and J. Vossen, Academic Press Inc., Vol. 16, 271 (1992).
5. T. Krug, *Barrier Pack 1990 Conference Proceedings*, London, England, The Packaging Group Inc. New Jersey, USA.
6. P. Mercea, L. Muresan, V. Mecea, D. Silipas and I. Ursu, *Journal of Membrane Science*, 35, 291 (1988).
7. S.W. Ing, Jr., R.E. Morrison, and J. E. Sandor, *Journal of the Electrochemical Society*, Vol 109, No. 3, 221 (1962).



JF87

Figure 8 - Transparent Barrier Coating Model